FULL-DUPLEX CHANNEL ANALYSIS FOR UNDERWATER ACOUSTIC COMMUNICATIONS

Cornelius Healy[a], Bilal Jebur[b], Charalampos Tsimenidis[a], Jeff Neasham[a], Jonathon Chambers[c]

[a] School of Engineering, Newcastle University, Newcastle upon Tyne, UK
[b] College of Electronics Engineering, Ninevah University, Mosul, Iraq
[c] Department of Engineering, University of Leicester, Leicester, UK

Cornelius Healy, School of Engineering, Newcastle University, Newcastle upon Tyne, UK, cornelius.healy@newcastle.ac.uk

Abstract: *The limited bandwidth available in underwater acoustic communication channels motivate the investigation of multiple access methods that maximize the capacity, such as full-duplex (FD) operation that can approximately double capacity. This paper presents characterization results of the self-interference (SI) channel from experimental data obtained by sea trials in the North Sea. Two scenarios are considered, i.e. hard and soft sea bottom with water column depths of 50 m. Initial results indicate that the delay spread of the local reverberation can extend up to 1.5 s before it reaches the noise floor level. This in turn has significant implications on the required hardware complexity of the SI mitigation methods based on adaptive filter echo cancellation, which will require tens of thousands of filter taps to deal with this delay spread range and prolonged training periods. Furthermore, the achievable range of the FD-based communication links will be affected by the levels of SI present in these channels, therefore, the results and channel modelling presented in this paper will be useful to FD modem designers.*

Keywords: *Underwater acoustic communication, In-band full-duplex communication, Acoustic measurements.*

INTRODUCTION

The potential to theoretically double the system throughput makes FD mode operation attractive in the severely impaired underwater acoustic channels. However, the close proximity of the concurrently active transducer and hydrophone will inevitably lead to large scale SI, relative to the desired distant signal. To realise a practical FD system, it will therefore be necessary to develop mitigation strategies to deal with the SI, both in the analog and digital domains. Development of these strategies will rely on accurate characterisation of the SI channel for real-world scenarios, to understand the behaviour and duration of the reverberations of the channel.

While FD communications has seen a great deal of interest in both wired and wireless radio frequency domains, significant work is still required on its application in underwater acoustic communications systems. The work in [1] presented early results on the feasibility of FD operation in underwater acoustic networking, with further developments on multi-user scenarios appearing in [2]. Hybrid SI interference suppression and cancellation techniques were considered in [3] for an OFDM system. In [4], an adaptive iterative scheme is proposed to deal with SI from the local channel along with inter-symbol interference. A recent work proposes novel MAC protocols for FD underwater acoustic networks [5]. Also recently published, the work in [6] considers the particular challenges of SI channel estimation in the FD underwater acoustic system and proposes a maximum likelihood based SI channel estimation algorithm with sparsity constraint. Most recently, the work in [7] proposes a digital-domain SI canceller which reconstructs the SI signal through use of the local transmit power amplifier (PA) output in a low-complexity adaptive filtering algorithm, improving the performance of the canceller by taking into account the nonlinearities introduced in the PA.

In this work, experimental measurements for the SI channel in a FD underwater acoustic communications system are presented. The characteristics of the channel are analysed and a simple model is proposed. This is key to understanding the challenges in developing techniques for a practical underwater acoustic system capable of FD operation. The rest of the paper is organised as follows: In Section 2, the details of the sea trial experiments are provided. Section 3 contains the channel measurements and related discussions, while Section 4 presents the proposed simplified channel model and demonstrates that it characterises the SI channel profile. Section 5 offers brief concluding remarks.

EXPERIMENTAL SETUP

Channel measurements were carried out in late August of 2018 in the North Sea at shallow water locations with depth approximately 50 m at two locations, with hard and soft sea bottoms. Fig. 1 provides the specification of the experiment, with the physical setup given in Fig. 1(a) outlining the channel geometry and defining a number of terms which will be used in later sections of the paper, and Fig. 1(b) provides the format of the transmitted signal used throughout the experiment, comprised of repeated Linear Frequency Modulated (LFM) chirp signals of increasing duration, followed by a number of pseudo-random binary sequences (PRSB) consisting of Binary Phase Shift Keying (BPSK) symbols modulated by m-Sequences of increasing chip length. The chirp signals had duration 0.1 s, 0.5 s and 1 s, respectively, while the PRSB signals used m-Sequences with chip length 2047, 4095 and 8191, respectively. The transmitted signals were separated by sufficiently large spacing to ensure that the reverberation effects of the channel could be observed.

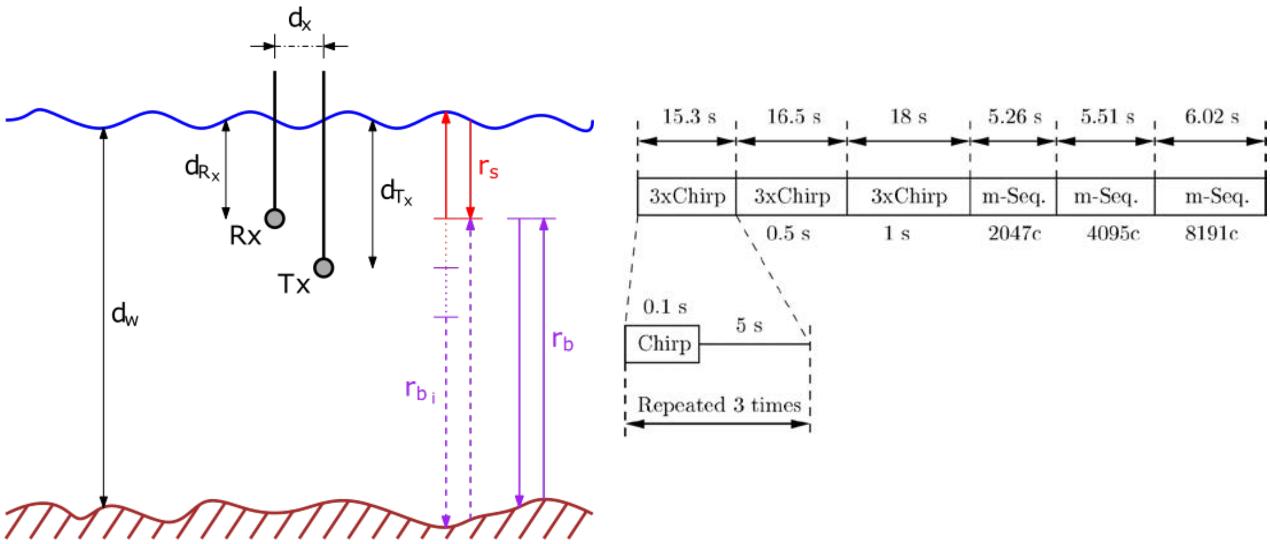

Fig. 1: Experimental setup (a) Channel geometry and (b) Signal format.

In the experiments, the receiver depth d_{Rx} was fixed for all measurements, while a number of different settings of transmitter depth d_{Tx} were taken. Two distinct settings of horizontal separation between transducer and hydrophone, d_x, were investigated, namely 0 m (no separation) and 1.2 m. As stated, the sea depth d_w was approximately 50 m throughout the experiment. For all measurements reported in this paper, the transducer and hydrophone were taken to be omni-directional, and no additional efforts were made to attenuate the signal between the transducer and hydrophone by means of absorbing material or baffle, so the presented measurements may be considered to constitute a worst-case scenario in terms of the SI reverberations. In future work the use of such physical SI suppression techniques will be considered.

Table 1 provides further details of the experimental parameters for the measurements presented in this work. Particularly notable are the transmitter depths for which the measurements were taken, and that during the experiment locations with both hard and soft sea bottom were encountered.

Parameter	Value
Centre Freq., BW	12 kHz, 8 kHz
Sampling Freq.	48 kHz
Source Level	170 dB
Signals	LFM Chirp / PRSB
R_x depth	5 m
T_x depth	6 m / 10 m / 15 m
Sea Bottom	Hard / Soft

Table 1: Experiment parameters.

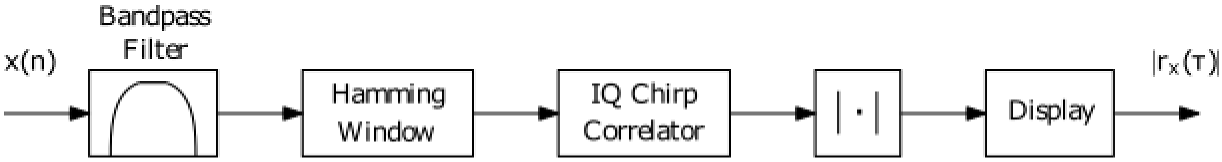

Fig. 2: Correlation processing chain on the measured SI signal.

CHANNEL MEASUREMENTS

In this section the measurements for the SI channel are presented, for a particular example of channel geometry and signal composition, as described in Fig. 1 and Table 1. In particular, the receiver depth was 5 m, transmitter depth 15 m, the sea bottom was soft and there was no separation between transmitter and receiver. The sea depth was approximately 52 m.

The correlation processing performed on the received SI signal from the channel is outlined in Fig. 2 for the LFM chirp signal. First, a band-pass filter is applied to the signal to remove observed noise contributions in the 18-20kHz range. Following this, a Hamming Window is applied to the signal, followed by the correlation operation and the magnitude of the output is used to produce the CIR plots shown in Fig. 3(a).

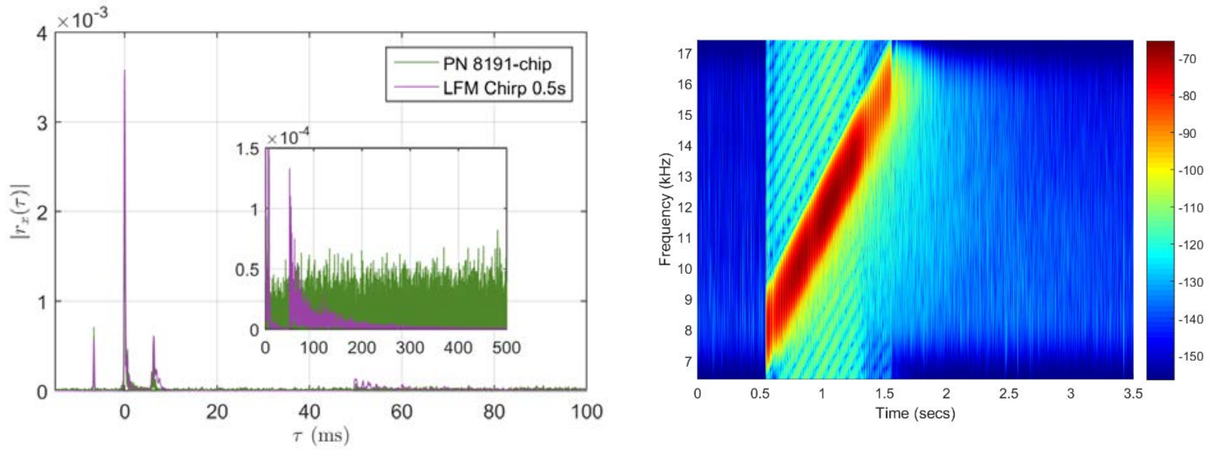

Fig. 3: Channel measurements (a) CIR for both chirp and PRBS and (b) Spectrogram.

In Fig. 3(a), two views of the produced CIRs are given. In the outer plot the shorter time scale view demonstrates the successful peaks corresponding to the direct path from transducer to hydrophone at zero delay, the first reflection from the sea surface after approximately 6.1 ms, and the first reflection from the sea bottom after approximately 50.2 ms. These values are consistent with the known geometry of the channel in Fig. 1(a) for speed of sound in water of approximately 1500 m/s. The outer plot demonstrates that both LFM chirp and PRBS signals can successfully extract these features from the signal. However, the larger time and smaller magnitude scale views shown in the inner plot demonstrate that the large side lobes of the m-Sequence autocorrelation obscure the finer details of the reverberation. Thus, for the following section, the LFM chirp signals will be the sole focus. A final note is needed on the peak which appears prior to the direct path peak. This peak is consistently observed throughout the recordings, and is believed to result from electromagnetic coupling. In Fig. 3(b), the spectrogram of a received signal for a 1 s LFM chirp is provided. This gives a clear visual demonstration of the long reverberations in the SI channel, which can be seen to extend well beyond one second. This will prove a significant challenge in implementing practical systems.

SIMPLE CHANNEL MODEL

In this section the simplified model for the SI channel is presented. Taking the well-known transmission loss model for acoustic waves in sea water, and accounting for non-ideal reflection losses at the sea bottom, a simple expression for the channel impulse response of the SI channel is proposed, and comparisons with the measured response of the channel demonstrate that the reverberations of the SI channel are characterised well.

Transmission and reflection loss for the SI channel may be expressed in terms of range r as

$$TRL(r) = TL(r) + n(r)\, RL\,, \qquad (1)$$

where the transmission loss in sea water, *TL(r)*, is given by

$$TL(r) = A + \xi \log_{10}(r) + \alpha(f) r\,, \qquad (2)$$

and the loss for each reflection from the sea bottom is

$$RL = 20 \log_{10}(\beta)\,, \qquad (3)$$

where β is the reflection coefficient, and is taken here to be 0.96. The term $n(r)$ in (1) accounts for the number of sea bottom reflections undergone by the acoustic wave after it has propagated range r can be found according to

$$n(r) = k + \left\lfloor \frac{r}{2\, d_w} \right\rfloor, \qquad (4)$$

where the operator $\lfloor x \rfloor$ denotes the largest integer smaller than x, and the term k is 0 for the acoustic waves which initially propagated in the upward direction, and 1 for those waves initially propagating downward.

From the geometry shown in Fig. 1, following the arrival of the acoustic wave taking the direct path from transducer to hydrophone, distinct arrivals occur for two sets of wave fronts, those initially propagating upwards and downwards, respectively. For the upward wave, in the notation of Fig. 1, arrivals will occur after the wave has travelled ranges

$$r = \{ r_s, (r_s + r_b), (2\, r_s + r_b), 2(r_s + r_b), (3\, r_s + 2\, r_b), \ldots \}, \qquad (5)$$

with each additional term occurring after an additional surface or bottom reflection. Likewise, for the initially downward propagating wave front, distinct arrivals after the direct path peak occur for ranges

$$r = \left\{ r_{b_i}, \left(r_{b_i} + r_s \right), \left(r_{b_i} + r_s + r_b \right), \left(r_{b_i} + 2\, r_s + r_b \right), \left(r_{b_i} + 2\, r_s + 2\, r_b \right), \left(r_{b_i} + 3\, r_s + 2\, r_b \right), \ldots \right\}. \qquad (6)$$

The above equations, along with the frequency-dependent attenuation factor and related terms below comprise a simple model for the SI channel reverberations, assuming lossless reflection at the sea surface and in the absence of small-scale diffusion effects. Nevertheless, the comparison between this model and the measured channel CIR in Fig. 4 demonstrates that this simple model captures the large-scale behaviour of the reverberations quite well.

In (2), the term A combines the attenuation effects of transducer and hydrophone in the plane of transmission/reception, the term ξ is the spreading factor, $\xi = 15$ for practical spreading, and $\alpha(f)$ is the frequency-dependent attenuation factor for transmission in sea water, given by [8]

$$\alpha(f) = a\,f^2 + \frac{b\,f_0}{1 + \left(\frac{f_0}{f}\right)^2} + \frac{c\,f_1}{1 + \left(\frac{f_1}{f}\right)^2}, \qquad (7)$$

$$a = 1.3 \times 10^{-7} + 2.1 \times 10^{-10}\,(T - 38)^2$$
$$b = 2S\ \times 10^{-5} \qquad c = 1.2\ \times 10^{-4} \qquad (8)$$
$$f_0 = 50\,(T + 1) \qquad f_1 = 10\,\frac{T - 4}{100}$$

The model described in (1)-(4) is presented in Fig. 4(a), which compares the transmission loss only case to that with both transmission and reflection losses. Fig. 4(b) demonstrates the fit achieved to the measured SI channel CIR, for the hard (HB) and soft (SB) sea bottom scenarios with transducer at 15 m and hydrophone at 5 m and no horizontal separation (d_x=0). The inner plot demonstrates that the transmission loss alone is sufficient in the short delay scale with the updated model of (1) not having a large effect. In the outer plot, the transmission loss only model deviates significantly at large delay for both scenarios. The proposed model better describes the observed CIR at the long delay range by taking into account the loss in reflection, with a very close match to the behaviour observed for the hard bottom, showing a small gap in the medium delay range for the soft bottom scenario.

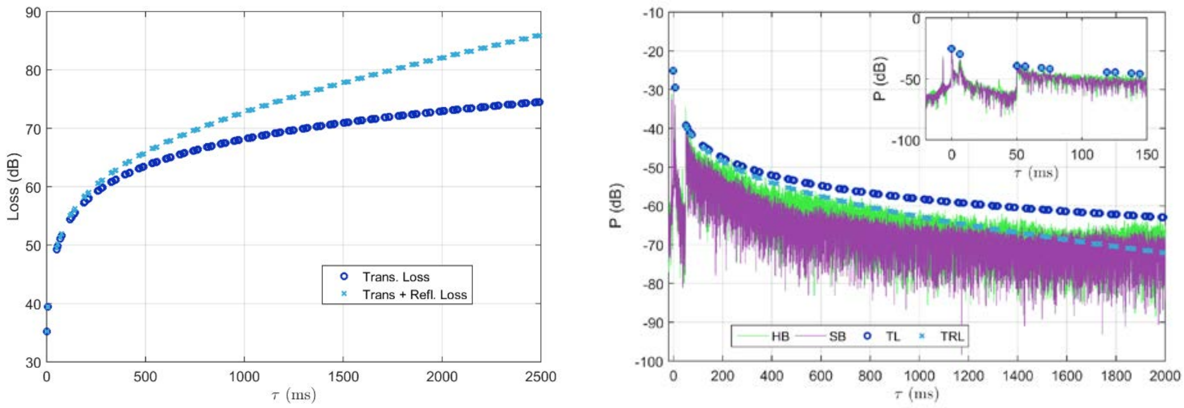

Fig. 4: Channel model (a) Transmission/reflection loss model and (b) Fit to the observed CIR.

CONCLUSIONS

In this paper the measurements for the SI channel in a FD system were presented for a number of shallow water scenarios. It was demonstrated through the use of CIRs and the received signal spectrogram that the reverberations in the SI channel persist for beyond 1 s in shallow water environments. A simple model was then introduced to characterise the taps of the SI channel CIR by taking into account sea water transmission loss and losses in reflection at the sea bottom. The model was demonstrated to accurately describe the behaviour of the SI channel. The results presented will inform future work on development of SI suppression and cancellation techniques for practical systems.

ACKNOWLEDGEMENTS

This work was supported by the EPSRC under project EP/R002665/1, Full-Duplex for Underwater Acoustic Communications. The authors would like to thank the Research Council for this funding.

REFERENCES

[1] **G. G. Xie, J. H. Gibson, and K. Bektas**, Evaluating the feasibility of establishing full-duplex underwater acoustic channels, In *Proc. of the Third Annual Mediterranean Ad Hoc Networking Workshop*, 2004.
[2] **G. Qiao, S. Liu, Z. Sun, F. Zhou**, Full-duplex, multi-user and parameter reconfigurable underwater acoustic communication modem, In *OCEANS 2013 – San Diego*, 2013.
[3] **L. Li, A. Song, L. J. Cimini, X.-G. Xia and C.-C. Shen**, Interference cancellation in in-band full-duplex underwater acoustic systems, In *OCEANS 2015 - Washington*, 2015.
[4] **J. Tian, S. Yan, L. Xu and J. Xi**, A time-reversal based digital cancelation scheme for in-band full-duplex underwater acoustic systems, In *OCEANS 2016 - Shanghai*, 2016.
[5] **F. Qu, H. Yang, G. Yu and L. Yang**, In-band full-duplex communications for underwater acoustic networks, *IEEE Network*, volume (32), pp. 59-65, 2017.
[6] **G. Qiao, S. Gan, S. Liu and Q. Song**, Self-interference channel estimation algorithm based on maximum-likelihood estimator in in-band full-duplex underwater acoustic communication system, *IEEE Access*, volume (6), pp. 62324-62334, 2018.
[7] **L. Shen, B. Henson, Y. Zakharov and P. Mitchell**, Digital self-interference cancellation for full-duplex underwater acoustic systems, *IEEE Trans. Circuits and Systems II: Express Briefs*, pp. 1-1, 2019.
[8] **R. Coates**, Underwater acoustic systems, *Macmillan new electronic series, Macmillan, 1990.*